Inorganic Chemistry
Article

Inorg. Chem. **2010**, *49*, 6525–6534 **6525**
DOI: 10.1021/ic1003148

Mechanism of Cadmium Ion Substitution in Mammalian Zinc Metallothionein and Metallothionein α Domain: Kinetic and Structural Studies

John Ejnik,[†,‡] C. Frank Shaw, III,[†,§] and David H. Petering*[,†]

Department of Chemistry, University of Wisconsin—Milwaukee, Milwaukee, Wisconsin 53201, Department of Chemistry, University of Wisconsin—Whitewater, Whitewater, Wisconsin, and Department of Chemistry, Illinois State University, Normal, Illinois. [†]University of Wisconsin—Milwaukee. [‡]University of Wisconsin—Whitewater. [§]Illinois State University

Received February 15, 2010

Cellular metallothionein (MT) protects against Cd^{2+} exposure through direct binding of the metal ion. The model reaction between rabbit liver Zn_7-MT-2 with Cd^{2+} was studied with stopped flow kinetics. Four kinetic steps were observable. Comparison of this reaction with an analog utilizing the MT Zn_4-α domain revealed that only the fastest step involved the Zn_3-β domain. Each step of the Zn_4-α domain reaction with Cd^{2+} displayed hyperbolic dependence of the observed rate constant on Cd^{2+} concentration, with the first step comprising 50% of the total reaction and each of the other two, 25%. The two constants extracted from each of these relationships were interpreted as the equilibrium constant for the initial binding of Cd^{2+} to the $Zn_{(4-n)}Cd_n$−thiolate cluster ($n = 0-3$) of the α domain and the first order rate constant for the exchange of Cd^{2+} for Zn^{2+} in the cluster. Activation enthalpies and entropies were determined for each constant. A suite of $Zn_{(4-n)}Cd_n$−thiolate clusters ($n = 0-3$) was prepared by titration of the Zn_4-α domain with $^{113}Cd^{2+}$. The products were analyzed by one-dimensional $^{113}Cd^{2+}$ NMR spectroscopy to define the distribution of $^{113}Cd^{2+}$ among the four cluster binding sites. Each of these species was also reacted with Cd^{2+}. The properties of these reactions were similar to those extracted from the reaction of Cd^{2+} with the overall domain. Thus, the kinetic results were linked to $^{113}Cd^{2+}$ occupancy among the cluster metal binding sites. In turn, this linkage permitted the interpretation of the various constants determined for the reaction of Cd^{2+} with the Zn_4-α domain in relation to the α domain cluster structure.

Introduction

Metallothioneins are widely distributed among organisms and are implicated in a variety of reactions and processes that involve metal ions and reactive electrophiles.[1−3] The mammalian protein is a small, sulfhydryl-rich molecule that binds multiple metal ions in two domains.[4−6] Its particular metal ion composition depends on the nature and history of the tissue source. Typically, Zn^{2+}, Cu^{1+}, or a mixture is found in the protein in the absence of exposure to toxic metals such as Cd^{2+}.[7−9] Zn-MT contains seven Zn^{2+} ions associated with 20 sulfhydryl (S) groups that are distributed in metal−thiolate clusters in the N-terminal, β (Zn_3S_9), and C-terminal, α (Zn_4S_{11}), domains.[4,6,10] [Abbreviations: α, C-terminal MT domain; β, N-terminal MT domain; M-MT, MT with 1−7 M^{2+} (Cd^{2+} and/or Zn^{2+}) bound to it; MT, metallothionein-MT-1 and MT-2 refer to isoforms; S, sulfhydryl or thiolate group.] Cd-MT has the same stoichiometry.[5,6] The interaction of the metal ions with the cysteinyl side chains results in the formation of two metal−thiolate clusters that serve as the interior of the two domains (Figure 1). As such, the particular metal ion−cysteine sulfhydryl connectivities determine the folding of each domain peptide about the cluster and, hence, the three-dimensional conformations of the two domains.

When Cd^{2+} enters cells containing basal Zn_7-MT, a sequence of reactions occurs that results in the steady state

*To whom correspondence should be addressed. E-mail: petering@uwm.edu.

(1) Petering, D. H.; Krezoski, S.; Tabatabai, N. M. *Met. Ions Life Sci.* **2009**, *5*, 353–398.
(2) Bell, S. G.; Vallee, B. L. *Chembiochem.* **2009**, *10*, 55–62.
(3) Cousins, R. J.; Liuzzi, J. P.; Lichten, L. A. *J. Biol. Chem.* **2006**, *281*, 24085–24089.
(4) Otvos, J. D.; Armitage, I. M. *Proc. Natl. Acad. Sci. U. S. A.* **1980**, *77*, 7094–7078.
(5) Arseniev, A.; Schultze, P.; Wörgötter, E.; Braun, W.; Wagner, G.; Vašák, M.; Kägi, J. H.; Wüthrich, K. *J. Mol. Biol.* **1988**, *201*, 637–657.
(6) Robbins, A. H.; McRee, D. E.; Williamson, M.; Collett, S. A.; Xuong, N. H.; Furey, W. F.; Wang, B. C.; Stout, C. D. *J. Mol. Biol.* **1991**, *221*, 1269–1293.
(7) Squibb, K. S.; Cousins, R. J.; Feldman, S. L. *Biochem. J.* **1977**, *164*, 223–228.
(8) Winge, D. R.; Geller, B. L.; Garvey, J. *Arch. Biochem. Biophys.* **1981**, *208*, 160–166.
(9) Chen, P.; Onana, P.; Shaw, C. F., 3rd; Petering, D. H. *Biochem. J.* **1996**, *317*, 389–394.
(10) Winge, D. R.; Miklossy, K. A. *J. Biol. Chem.* **1982**, *257*, 3471–3476.

Published on Web 06/18/2010

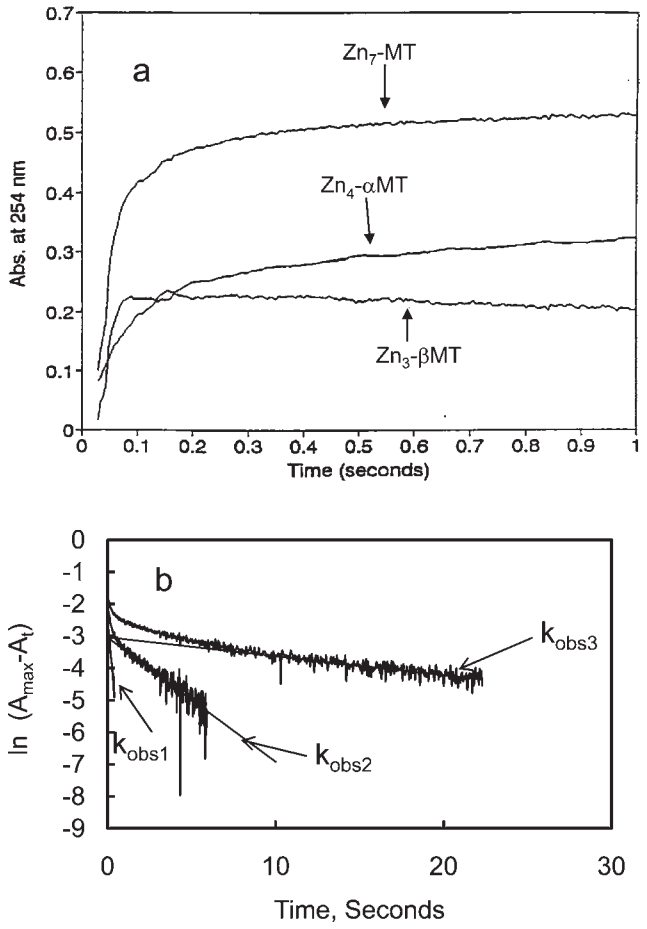

Figure 1. Metal exchange reaction between Zn_7-MT or Zn_4-αMT and Cd^{2+}. (a) Spectrophotometric analysis of the reaction between 10 μM Zn_7-MT or Zn_4-αMT and 800 μM Cd^{2+} in 10 mM Tris-Cl—pH 7.4, and 0.1 M KCl at 25° observed at 254 nm. The figure shows the difference in the time course for these two reactions which represents the reaction of the Zn_3-β domain with Cd^{2+}. (b) First order plot of data from the reaction of Zn_4-αMT with Cd^{2+} under the same conditions as in a.

appearance of the mixed metal species, $Cd_n,Zn_{(7-n)}$-MT (n = 1−7), in which each metal ion is uniquely distributed among the two clusters depending upon the value of n.[11] First, Cd^{2+} rapidly displaces Zn^{2+} from preexisting Zn-MT (reaction 1). Second, it induces the synthesis of additional apoMT that may react with Zn^{2+} prior to metal ion substitution by Cd^{2+} or directly react with Cd^{2+} to form Cd_7-MT.[12] Finally, the available reagents exchange metal ions to form the mixed metal species (reaction 2).[11] Cd^{2+} is complexed by apoMT, and additional Zn_7-MT has formed, the Zn and Cd proteins:

$$Zn_7\text{-MT} + 7Cd^{2+} \rightleftharpoons Cd_7\text{-MT} + 7Zn^{2+} \quad (1)$$

$$kZn_7\text{-MT} + mCd_7\text{-MT} \rightleftharpoons (k+m)Zn_{(7k/k+m)}, Cd_{(7m/k+m)}\text{-MT} \quad (2)$$

The incomplete titration of Zn_7-MT with Cd^{2+} does not yield the same mixed metal product as formed in reaction 2.[11] Instead, it produces a kinetically controlled product that rearranges to the product of reaction 2 upon mild heating.[13]

The present study was undertaken to understand the mechanism of reaction 1 as a prelude to investigating the more complicated interprotein metal ion exchange that takes place in the second reaction.

Methods

Metallothionein Preparation. Female white New Zealand rabbits (5 lbs) were injected with 2 mL of sterilized 0.15 M $ZnSO_4$, pH 6.0, every 24 h for 8 days. Then, the animals were euthanized and the livers removed and homogenized in 0.25 M sucrose, 6 mM 2-mercaptoethanol, and 5 mM Tris/Cl buffer, pH 8.0 (100 g in 200 mL of degassed solution). After centrifugation, the supernatant was chromatographed over a 12 × 85 cm Sephadex G-75 column equilibrated and eluted with an anaerobic buffer comprised of 5 mM Tris/Cl and 2 mM 2-mercaptoethanol, pH 8 at 4 °C.

The MT fractions detected by atomic absorption spectrophotometry were pooled, filtered through a 0.45 um nylon membrane, and purified further by HPLC on a 21.5 mm × 15 cm DEAE 5PW semipreparation ion exchange column. The protein and buffer solutions were filtered with 0.45 um nylon membrane filters, loaded onto the ion exchange column, and eluted with the following gradient of 5−300 mM Tris/Cl, pH 7.6, as follows:

time (min)	0	25	55	95	105	115
A (5 mM Tris/Cl, pH 7.6)	100	100	92	0	0	100
B (300 mM Tris/Cl, pH 7.6)	0	0	8	100	100	0

Fractions were collected and the MT-1 and MT-2 isoforms identified by zinc atomic absorption spectroscopy and conductivity. MT-1 and MT-2 fractions were separately pooled and stored frozen for future use. MT-2 was used in all experiments conducted within this study.

Isolation of α Domain. A 9.1 μmol sample of Zn_7−MT-2 (0.76 mM Zn^{2+}) was used to prepare the α domain. Initially, 5.25 equiv of cadmium chloride per mol of MT were added to the sample and allowed to incubate for 15 min in order to displace Zn^{2+} primarily from the α domain.[11] Next, an 11-fold excess of EDTA (8.7 mM) and 1.6 mg of the protease subtilisin were added to the sample and allowed to incubate for 75 min. EDTA binds displaced Zn^{2+} and preferentially competes for residual Zn^{2+} bound in the β domain.[14] In this mixture, subtilisin degrades the apo-β domain, leaving a protease resistant Cd_4-α domain. The sample was acidified with HCl to a H^+ concentration of 0.2 N. The sample was chromatographed over a 3.5 cm × 25 cm column of G-15 Sephadex and then over a 3.5 cm × 30 cm G-50 Sephadex size exclusion column equilibrated with 0.05 N HCl. Fractions were collected and their absorbance at 220 nm measured. Some holoprotein remained that eluted first. The second peak at a molecular weight of 3000 was pooled. To the pooled fractions, 9 mM $ZnSO_4$ or $CdCl_2$ was added, and the pH was raised to 7.4 with a solid Trizma base. The sample was then concentrated with a YM1 amicon membrane. The resultant sample was desalted with a 3.5 cm ×24 cm G-15 Sephadex column equilibrated with 5 mM Tris/Cl—pH 7.4. The first peak was pooled as the α domain. The α domain was characterized by measuring the SH to zinc ratio as described for Zn_7MT. Ultimately, the α domain was also characterized by solving the 3-D solution structure of the domain.[19] The results showed that its preparation led to a single product. Then, a ^{111}Cd-treated sample was identified as the $^{111}Cd_4$-αMT-2 sample by ^{111}Cd 1-D NMR spectroscopy, as described below.

(11) Nettesheim, D. G.; Engeseth, H. R.; Otvos, J. D. *Biochemistry* **1985**, *24*, 6744–6751.
(12) Winge, D. R.; Premakumar, R.; Rajagopalan, K. V. *Arch. Biochem. Biophys.* **1975**, *170*, 242–252.
(13) Stillman, M. J.; Cai, W.; Zelazowski, A. J. *J. Biol. Chem.* **1987**, *262*, 4538–4548.
(14) Nielson, K. B.; Winge, D. R. *J. Biol. Chem.* **1983**, *258*, 13063–13069.

Kinetics of the Reaction of Zn_4-αMT with Cd^{2+}. The kinetics of metal exchange between Zn_4-αMT and Cd^{2+} were studied under pseudo first-order conditions for [Cd^{2+}]. An updated Durram stopped-flow instrument was used to measure the UV absorbance change at 254 nm from the reaction of Zn_4-αMT with Cd^{2+}.[15] The dead-time of the instrument was 5 ms, determined by calibration with the reaction of ferricyanide and ascorbate. The temperature of the stop flow was calibrated with an automated water bath and thermometer. The stopflow cell and sample syringes were submerged in the water bath.

A solution of 10 μM Zn_4-αMT and Cd^{2+} concentrations of 200, 400, 800, 1600, and 2400 μM were reacted at 11°, 25°, and 36 °C in 0.1 M KCl and a 10 mM Tris/Cl—pH 7.4 buffer. The UV absorbance was measured for 80 s with data points taken every 5 ms. The cumulative data were analyzed on the basis of a model with triple concurrent pseudo first-order reactions leading to the same product. Since the change in absorbance provided a direct measurement of the overall extent of the reaction, the following equation was used:

$$A_t = A_i + A_1(1 - \exp(-k_{obs1}t)) + A_2(1 - \exp(-k_{obs2}t)) + A_3(1 - \exp(-k_{obs3}t) \quad (3)$$

$$A_t = A_1 \exp(k_{obs1}t) + A_2 \exp(k_{obs2}t) + A_3 \exp(k_{obs3}t) \quad (4)$$

where A_i represents the absorbance at time zero; A_1, A_2, and A_3 represent the absorbances of the reactants which are proportional to their respective concentrations; and k_{obs1}, k_{obs2}, and k_{obs3} represent the observed rate constants for the three phases of the reaction. The first of these, eq 3, describes the decay kinetics of a reaction and the second, eq 4, its formation kinetics. Using eq 4, the observed rate constants and respective maximum absorbances for the component reactions were extracted using the curve fit program TableCurve 2D from Jandel Scientific. Data processing for eq 3 was done with Quattro Pro. The k_{obs} versus [Cd^{2+}] plot for each rate process was described by a hyperbola. This type of rate behavior is most simply explained by a two-step reaction with an element of reversibility.[16] Using an equation for a hyperbola ($y = ax/(b + x)$), the constants a and b were determined using the curve fit program TableCurve 2D from Jandel Scientific.

Kinetics of the Reaction of Zn_7MT-2 with Cd^{2+}. The kinetics of the metal exchange between Zn_7-MT and Cd^{2+} were studied under pseudo first-order conditions of Cd^{2+}, as above. A solution of 10 μM Zn_7-MT and Cd^{2+} concentrations of 200, 400, 800, 1600, and 2400 μM were reacted at 11°, 25°, and 36 °C in 0.1 M KCl and a 10 mM Tris/Cl—pH 7.4 buffer. The UV kinetic data were analyzed on the basis of a model with four concurrent pseudo first-order reactions leading to the same product. Since the change in absorbance provided a direct measurement of the overall extent of the reaction, a modification of eq 3 can be used:

$$A_t = A_i + A_1(1 - \exp(-k_{obs1}t)) + A_2(1 - \exp(-k_{obs2}t)) + A_3(1 - \exp(-k_{obs3}t)) + A_4(1 - \exp(-k_{obs4}t)) \quad (4a)$$

where A_i represents the absorbance at time zero; A_1, A_2, A_3, and A_4 represent the final absorbances of the products which are proportional to their respective concentrations; and k_{obs1}, k_{obs2}, k_{obs3}, and k_{obs4} are the observed rate constants for the several phases of reaction.

The absorbance changes were consistent with four phases to the reaction, the fastest attributable to the reaction of Zn_3-βMT with Cd^{2+}. In order to obtain the kinetic information for this part of the reaction, the UV kinetic data for the reaction of defined concentrations of Cd^{2+} with Zn_4-αMT were subtracted from the corresponding data for the Zn_7-MT reactions. The remainder of the reaction was analyzed with TableCurve 2D as above.

Activation Parameters for the Reactions of Zn_7-MT and Zn_4-αMT with Cd^{2+}. The activation parameters for the metal exchange reaction between Zn_7-MT and Cd^{2+} were obtained from kinetic results obtained at 11, 25, and 36 °C, using the same experimental regime as described above. The activation parameters were determined from plots of $\ln(k/T)$ versus $1/T$, where k is the rate constant and T is temperature in degrees Kelvin.[17] The plot of $\ln(k/T)$ versus $1/T$ is linear, with a slope $-\Delta H^{\ddagger}/R$ and an intercept $(23.8 + \Delta S^{\ddagger}/R)$, in which $\Delta H^{\ddagger}$ and $\Delta S^{\ddagger}$ are the enthalpy and entropy of activation, respectively. The free energy of activation $\Delta G^{\ddagger}$ was calculated from the equation, $\Delta G^{\ddagger} = \Delta H^{\ddagger} - T\Delta S^{\ddagger}$.

Kinetics of the Reaction of Zn_7-MT with Cd^{2+} Monitored with Zincon. The kinetics of the metal ion exchange between Zn_7-MT and Cd^{2+} were studied under pseudo first-order conditions for Cd^{2+}, using the metal binding ligand, zincon, to follow the displacement of Zn^{2+} in a non-rate-limiting process.[18] Zn−zincon formation was monitored at 620 nm and Cd−thiolate binding at 254 nm. Cd−zincon does not absorb at 620 nm. The reaction of 2 μM Zn_7-MT with a pseudo first-order concentration of 140 μM Cd^{2+} and 20 μM zincon was carried out at 25 °C in 0.1 M KCl and a 10 mM Tris/Cl—pH 7.4 buffer. The UV or visible absorbance changes were measured for 45 s with data points taken every 5 ms. The data were analyzed as above on the basis of the model of concurrent pseudo first-order reactions leading to the same product. The observed rate constants and respective absorbances were analyzed as previously described. The rate constants from the two kinetic reactions at 254 and 620 nm were compared to determine if the Cd−thiolate formation at 254 nm occurred at the same rate as zinc release at 620 nm.

Kinetics of the Reactions of Zn_4-αMT, Zn_3Cd_1-αMT, ..., Zn_1Cd_3-αMT with Cd^{2+}. The kinetics of the metal exchange between Zn_4αMT, Zn_3Cd_1αMT, ..., Zn_1Cd_3αMT, and Cd^{2+} were studied under pseudo first-order conditions for Cd^{2+}. Solutions of 10 μM proteins and pseudo first-order concentrations of 600 μM Cd^{2+} were reacted at 25 °C in 0.1 M KCl and a 10 mM Tris/Cl—pH 7.4 buffer. The UV kinetic absorbance spectra at 254 nm were measured for 80 s with data points taken every 5 ms. The UV kinetic data were analyzed as above based on a model with double concurrent, pseudo first-order rate processes leading to the same product in which each process accounts for the reaction of 2 Cd^{2+} ions. In so doing, the two slower steps of the triphasic reaction were aggregated. This simplification was based on the NMR titration finding that Cd^{2+} ions 1 and 2 randomly enter the same two cluster sites and that Cd^{2+} ions 3 and 4 occupy the two remaining sites. The changes in absorbance for the faster and slower processes for a series of reactions were measured in a series of reactions to assess a fraction of the reaction occurring in these kinetic processes.

Titration of Zn_4-αMT with $^{111}Cd^{2+}$ Monitored by ^{111}Cd NMR. A 2 mL Zn_4-αMT-2 (1 mM) sample was placed in a 10 mm tube with 20% D_2O as a frequency lock. The sample was titrated with four 13 μL aliquots of 0.136 M $^{111}Cd^{2+}$ and allowed to incubate for 30 min after each addition. Each aliquot represented 0.9 of the amount of Cd^{2+} needed for stoichiometric replacement of Zn^{2+}. Also, after each incubation was complete, 8.7 μL of 0.2 M

(15) Ejnik, J.; Robinson, J.; Zhu, J.; Försterling, H.; Shaw, C. F.; Petering, D. H. *J. Inorg. Chem.* **2002**, *88*, 144–152.

(16) Wilkins, R. G. *Kinetics and Mechanism of reactions of transition Metal Complexes*; VCH: New York, 1991; pp 23−25.

(17) Espenson, J. H. *Chemical Kinetics and Reaction Mechanisms*; McGraw-Hill Publishing Company: New York, 1981; pp 118−120.

(18) Shaw, C. F., III; Laib, J. E.; Savas, M.; Petering, D. H. *Inorg. Chem.* **1990**, *28*, 403–408.

(19) Ejnik, J. W.; Muñoz, A.; DeRose, E.; Shaw, C. F., 3rd; Petering, D. H. *Biochemistry* **2003**, *42*, 8403–8410.

EDTA was added to bind free Zn^{2+}. The NMR spectra were collected at 25 °C after each titration.

^{111}Cd NMR spectra were recorded at 106 MHz on a General Electric GN-500 spectrometer.[19] The broadband ^{1}H decoupler was on during data acquisition and off during the delay periods. The ^{1}H decoupling improved the spectral resolution by removing the unresolved proton couplings that originate from the scalar three-bond interaction between the β protons of the multiple cysteine ligands and the $^{111}Cd^{2+}$ ions. In the experiments, the pulse sequence consisted of a 15 μs pulse, an acquisition time of 168 ms, and a 400 ms delay time. A line-broading function of 30 Hz was applied before Fourier transformation. Chemical shifts were reported in parts per million downfield from the ^{111}Cd resonance of 0.1 M $^{111}Cd(ClO_4)_2$ in D_2O. The spectral width was 16 000 Hz.

Data Analysis. All kinetic experiments were done five times and the results reported as averages ± standard deviation of the mean.

Results

Kinetics of the Reaction of Zn_4-αMT with Cd^{2+}. The kinetics of the metal exchange between Zn_4-αMT and Cd^{2+} were studied under pseudo first-order conditions at 25 °C. The metal exchange reaction between Zn_4-αMT and Cd^{2+} was followed spectrophotometrically by monitoring the formation of Cd−thiolate bonds in Cd-MT at 254 nm (Figure 1a; Supporting Information Figures 1S, 2S). A plot of $\ln(A_t - A_i)$ versus time, in which A_i, the initial absorbance, is 0 and A_t is the absorbance at time t, was consistent with three concurrent pseudo first-order reactions leading to the same product, based on eq 4 (Figure 1b). The percent absorbance changes in phases 1, 2, and 3 were 50%, 25%, and 25% of the total, respectively. On the basis of the percent absorbance changes, two Zn^{2+} ions exchange with a single rate constant, k_{obs1}; the other two metals exchange with rate constants k_{obs2} and k_{obs3}.

The observed rate constants were extracted from the reaction of 10 μM Zn_4-αMT with pseudo first-order Cd^{2+} concentrations of 200, 400, 800, 1600, and 2400 μM at 25 °C, with curve fitting software based on eq 3 (Table 1). Plots of each k_{obs} versus $[Cd^{2+}]$ revealed that the two faster rate processes were characterized by a hyperbolic dependence of the rate constant upon the $[Cd^{2+}]$ hyperbola ($y = ax/(b + x)$), where $a = k$ and $b = K_d$ in reactions 5 and 6 (Figure 2 for k_{obs1}; Supporting Information Figures 3S and 4S). The slowest rate process appeared linear. Nevertheless, assuming all the steps followed the same mechanism, a curve-fitting program assigned the constants "a" and "b" as 51 s^{-1}, 3.0 s^{-1}, 2.3 s^{-1} and 0.21 mM, 0.25 mM, and 0.91 mM, respectively, to the rate processes described by k_{obs1}, k_{obs2}, and k_{obs3} (Table 2).

A simple mechanism accounting for the kinetics of each phase is one with two consecutive reactions including one reversible step:

$$A + B \rightleftharpoons A\cdot B \quad K_d \tag{5}$$

$$A\cdot B \rightarrow C + D \quad k \tag{6}$$

in which A is Zn-MT, B is Cd^{2+}, and A·B is Cd−Zn-MT. Therefore, the data for each rate process fit the empirical equation:

$$k_{obs} = k[Cd^{2+}]/(K_d + [Cd^{2+}]) \tag{7}$$

Table 1. Observed Rate Constants, k_{obs}, for the Pseudo First-Order Reactions of Zn_4-αMT with Cadmium at Temperatures of 11, 25, and 36° C[a]

Zn_4-αMT at 11 °C			
[cadmium]	k_{obs1} (s^{-1})	k_{obs2} (s^{-1})	k_{obs3} (s^{-1})
0.200 mM	0.78 ± 0.10	0.065 ± 0.005	0.012 ± 0.002
0.400 mM	1.3 ± 0.3	0.11 ± 0.01	0.019 ± 0.002
0.800 mM	2.5 ± 0.3	0.17 ± 0.04	0.036 ± 0.002
1.60 mM	4.7 ± 0.4	0.29 ± 0.04	0.067 ± 0.003
2.40 mM	6.3 ± 0.5	0.40 ± 0.05	0.095 ± 0.005
Zn_4-αMT at 25 °C			
[cadmium]	k_{obs1} (s^{-1})	k_{obs2} (s^{-1})	k_{obs3} (s^{-1})
0.200 mM	4.5 ± 0.2	0.27 ± 0.05	0.054 ± 0.004
0.400 mM	7.8 ± 1.1	0.47 ± 0.07	0.10 ± 0.01
0.800 mM	13 ± 2	0.67 ± 0.06	0.19 ± 0.01
1.60 mM	23 ± 3	1.1 ± 0.1	0.35 ± 0.01
2.40 mM	26 ± 2	1.5 ± 0.1	0.49 ± 0.01
Zn_4-αMT at 36 °C			
[cadmium]	k_{obs1} (s^{-1})	k_{obs2} (s^{-1})	k_{obs3} (s^{-1})
0.200 mM	11 ± 1	0.92 ± 0.10	0.15 ± 0.02
0.400 mM	18 ± 2	1.4 ± 0.2	0.31 ± 0.02
0.800 mM	32 ± 2	2.3 ± 0.2	0.62 ± 0.03
1.60 mM	43 ± 4	3.2 ± 0.3	1.1 ± 0.2

[a] Reaction conditions: 10 μM Zn_4-αMT, 10 mM Tris/Cl—pH 7.4, 0.1 M KCl.

in which the constants k and K_d are listed in Table 2. If the first reversible step is the more rapid one, A·B will be in equilibrium with A and B throughout the reaction and the rate of product formation will be equal to the rate of loss of A + A·B or the gain of C (Cd-MT) in eqs 6 and 7.

Kinetics of the Reaction of Zn_7-MT with Cd^{2+}. The kinetics of the metal ion exchange between Zn_7-MT and Cd^{2+} were studied spectrophotometrically under pseudo first-order conditions at 25 °C as with Zn_4-αMT. The time-dependent changes in absorbance were analyzed in terms of four concurrent pseudo first-order reactions leading to the same product based on eq 5. The percent absorbance changes in A_1, A_2, A_3, and A_4 were 41%, 29%, 15%, and 15%, respectively. On the basis of the percent absorbance changes, three metal ions exchanged with the rate constant k_{obs1}, two metal ions with k_{obs2}, and one each with k_{obs3} and k_{obs4}. Comparison of the kinetic results with those of Zn_4-αMT indicated that the processes represented by k_{obs2}, k_{obs3}, and k_{obs4} belonged to the α domain (Figure 1a). The remainder of the reaction was ascribed to the β domain. Quantitative rate expressions for that part of the reaction contributed by the α domain were obtained from the study with Zn_4-αMT.

Observed rate constants for reaction of the β domain as a function of Cd^{2+} concentration were determined after subtracting out the contribution of the α domain to the overall reaction, using the data from the reaction of the isolated Zn_4- αMT with Cd^{2+} as described in the Methods. A plot of k_{obs1} versus $[Cd^{2+}]$ yielded a straight line with the intercept passing through zero at all temperatures. The slope was determined to be 75 000 M^{-1} s^{-1}

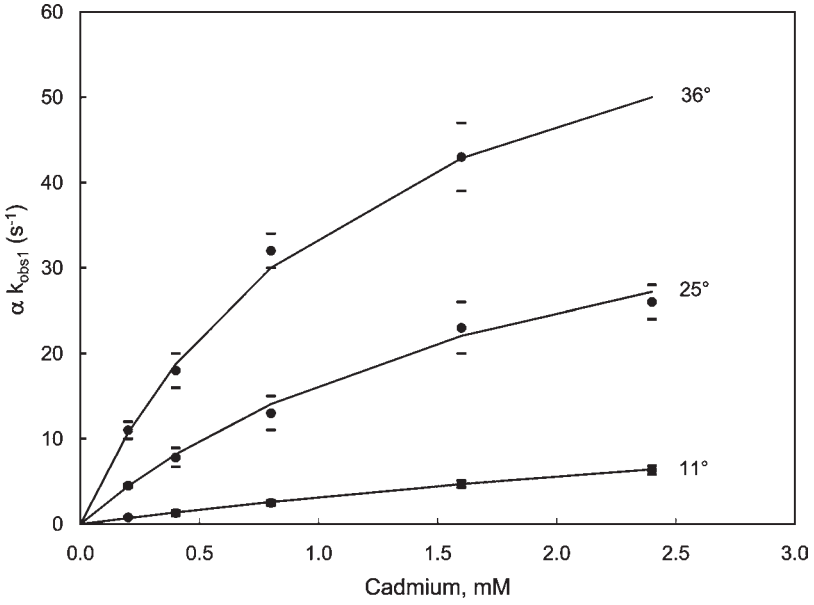

Figure 2. Plot of k_{obs1} (Table 1) versus [Cd^{2+}] for the reaction of Zn_4-α domain with Cd^{2+} at 11°, 25°, and 36 °C.

Table 2. Reaction Constants for the Reaction of Cd^{2+} with Zn_7-MT[a]

	Zn_4-αMT		
	11 °C	25 °C	36 °C
	rate constant (s^{-1})		
k_1	24	51	75
k_2	0.96	3.0	5.3
k_3	0.47	2.3	6.2
	dissociation constant (M^{-1}) × 10^4		
K_{diss1}	6.6	2.1	1.2
K_{diss2}	3.4	2.5	1.0
K_{diss3}	10	9.1	7.1
	β Domain of Zn_7-MT		
	11 °C	25 °C	36 °C
	rate constant (M^{-1} s^{-1})		
k_β	26000	75000	160000

[a] Reaction conditions: 10 μM Zn_7-MT, 10 mM Tris/Cl—pH 7.4, 0.1 M KCl.

for the k_{obs1} step at 25 °C (Table 3; Supporting Information Figure 5S) .

$$k_{obs} = k[Cd^{2+}] \quad (8)$$

A single second-order reaction described the reaction process as

$$A + B \xrightarrow{k} C \quad (9)$$

Therefore, the data fit the empirical equation

$$Vel = k[Cd^{2+}][ZnMT] \quad (10)$$

The second-order rate constant k is listed in Table 2.

Table 3. Observed Rate Constants, k_{obs1}, for the Pseudo First-Order Reactions of the β Domain of Zn_7-MT with Cd^{2+} at Temperatures of 11, 25, and 36° C[a]

	k_{obs1} (s^{-1})		
[cadmium]	11 °C	25 °C	36 °C
0.200 mM	5.0 ± 0.5	17 ± 2	40 ± 10
0.400 mM	9 ± 1	30 ± 4	70 ± 10
0.800 mM	20 ± 2	65 ± 6	130 ± 20
1.60 mM	40 ± 5	120 ± 10	250 ± 20
2.40 mM	63 ± 5	180 ± 20	

[a] Reaction conditions: 10 μM Zn_7-MT, 10 mM Tris/Cl—pH 7.4, 0.1 M KCl.

Activation Parameters from the Rate Constants for the Reaction of Zn_4-αMT with Cd^{2+}. The activation parameters of the metal ion exchange between Zn_4-αMT and Cd^{2+} were calculated on the basis of kinetic data acquired at 11, 25, and 36 °C using plots of $\ln(k/T)$ versus $1/T$ (Table 2 and Figure 3), where k is the rate constant and T is the temperature in degrees Kelvin. The activation parameters of the rate processes for the α domain (k_1, k_2, k_3) were calculated from results of the reaction of the isolated α domain with Cd^{2+} and those related to k_β from the reaction of the holoprotein with Cd^{2+} (Table 4). The activation enthalpy more than doubled in the progression of phases 1−3. Similarly, the entropy of activation increased in the same sequence. The β domain's enthalpy of activation was larger than those for the α domain's k_1 and k_2 and smaller than that for k_3. The free energy of activation increased sharply from the β domain reaction to the α domain's three phases, consistent with the relative velocities of these reaction phases. The compensatory behavior of activation enthalpy and entropies in the α domain reaction resulted in a free energy of activation that was not strongly dependent upon temperature.

The second parameter extracted from the kinetics is attributed to the thermodynamic dissociation constant of reaction 5. Although K_d for the slowest phase of reaction is the largest at each temperature, the

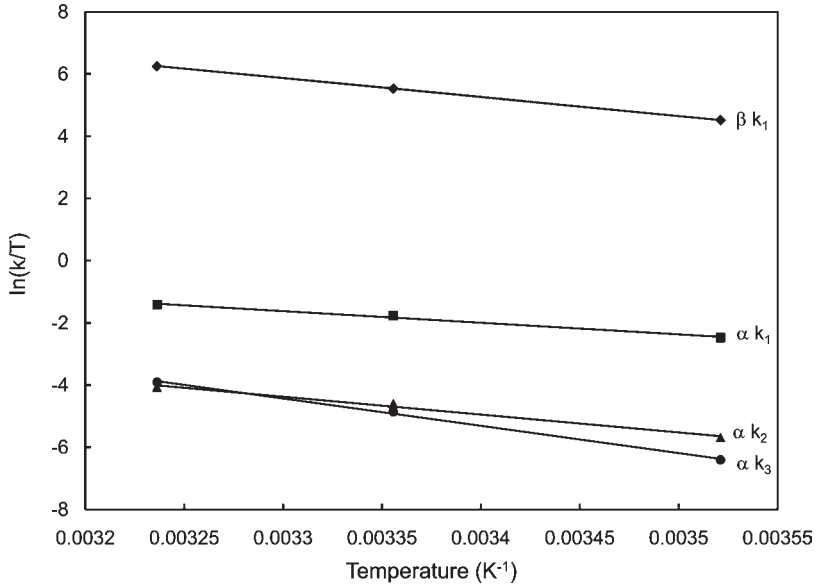

Figure 3. A plot of $\ln(k_{obs}/T)$ versus $1/T$ data in Table 2 to obtain activation parameters for the reaction of Zn_4-αMT with Cd^{2+}.

Table 4. List of Activation Parameters from the Reaction of Zn_7-MT with Cd^{2+}[a]

	α domain			β domain
	k_1	k_2	k_3	$k_{1\beta}$
$\Delta H^{\ddagger}$ (kJ/mol)	31	48	73	51
$\Delta S^{\ddagger}$ (J/mol·K)	−110	−77	6.5	18
$\Delta G_{298}^{\ddagger}$ (kJ/mol)	64	71	74	46
	K_{d1}	K_{d2}	K_{d3}	
ΔG_{298} (kJ/mol)	−15	−15	−12	

[a] Reaction conditions: 10 μM Zn-MT, 10 mM Tris/Cl—pH 7.4, 0.1 M KCl.

differences are relatively small as emphasized by the similar standard state free energies calculated from the K_d data.

Kinetics of the Reaction of Zn_4-MT with Cd^{2+} Monitored with Zincon. It was important to determine that the rate profile observed by following Cd−thiolate bond formation at 254 nm represented the full metal exchange process. Therefore, the rate of Zn^{2+} displacement from Zn_4-MT was directly compared with the rate of Cd−thiolate bond formation, using zincon to bind Zn^{2+} released from MT. The time-dependent absorbance change at 254 nm (Cd−thiolate bond formation) for the fastest phase of the reaction was compared to the absorbance increase at 620 nm (Zn−zincon formation) for the same reaction monitored with zincon (Figure 4). The k_{obs} was $4.0 \pm 0.5\ s^{-1}$ when monitored at 254 nm and $3.5 \pm 0.5\ s^{-1}$ for observations at 620 nm. Since there is experimentally no difference in these k_{obs} values, Cd−thiolate bond formation occurred at the same rate that Zn^{2+} was released from MT-2. On the basis of the discussion related to eqs 5−7, the kinetics observed at 254 nm follow Cd-MT product formation and should agree with those that track the release of Zn^{2+}. The fact that these two measurements agree supports the conclusion that the rate of $Cd^{2+}-Zn^{2+}$ thiolate bond exchange monitored at 254 nm represents the limiting rate of the overall metal ion exchange reaction.

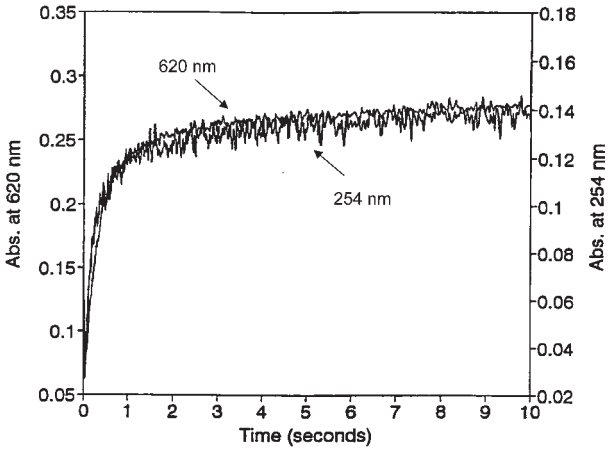

Figure 4. Reaction of Zn_4-αMT with Cd^{2+}: comparison of the absorbance change of the metal exchange monitored at 254 nm (Cd−thiolate bond formation) and at 620 nm (Zn−zincon formation). Conditions: 10 mM Tris-Cl—pH 7.4, and 0.1 M KCl at 25°; 2 M Zn_4-αMT and 140 μM Cd^{2+} with 20 μM zincon in one of the reactions.

Titration of Zn_4-αMT with $^{111}Cd^{2+}$ Monitored by ^{111}Cd NMR. Zn_4-αMT was titrated with $^{111}Cd^{2+}$ to make a series of mixed metal species that would serve as hypothetical intermediates in the reaction of Cd^{2+} with Zn_4-αMT. Thus, $Zn_3{}^{111}Cd_1$-αMT, ..., $Zn_1{}^{111}Cd_3$-αMT were prepared and their distributions of $^{111}Cd^{2+}$ among metal ion binding sites of the cluster determined by 1-dimensional ^{111}Cd-NMR spectroscopy, on the basis of a previous analysis of this titration.[11] All observed resonances were assigned except two located between 670 and 650 ppm. Once in hand, this information was used to provide a structural interpretation of the results of the reactions between Cd^{2+} and $Zn_nCd_{(4-n)}$-αMT.

The addition of one equivalent of $^{111}Cd^{2+}$ per mole of Zn_4-αMT resulted in the appearance of two major peaks with chemical shifts of 647.2 and 613.1 ppm (Figure 5). These peaks were labeled 2 and 5, respectively. Otvos et al. previously defined the site distribution of Cd^{2+}.[11] On the basis of their experiments, the metal ion giving rise to

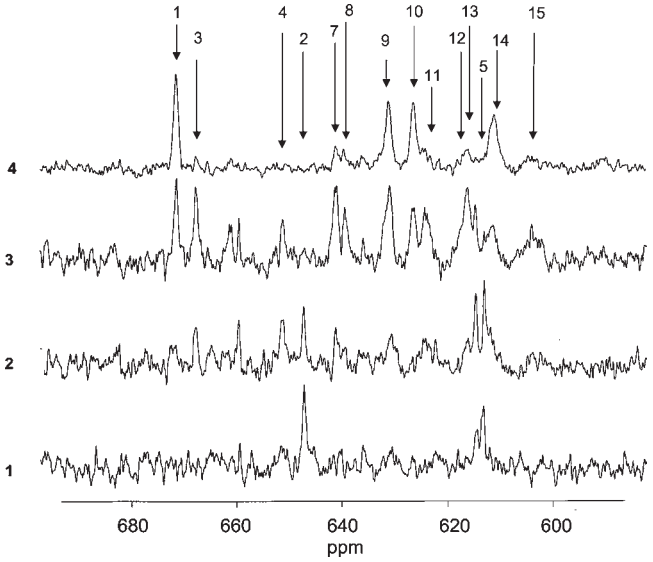

Figure 5. NMR spectroscopy titration of Zn_4-αMT with $^{111}Cd^{2+}$. Conditions: 1 mM Zn_4-αMT in 20% D_2O. Cadmium equivalents are labeled as 1−4 on the *y* axis.

peak 2 was assigned to site VI as Cd_1Zn_3-αMT and peak 5 to site V as Cd_1Zn_3-αMT of the ^{111}Cd NMR spectrum (Figure 6).[11] Two minor peaks also appear after the addition of one equivalent of $^{111}Cd^{2+}$ with chemical shifts of 651.45 and 614.74 ppm (4 and 13, respectively). These peaks show evidence of the presence of some Cd_2Zn_2-αMT cluster with Cd^{2+} located in sites VI and V. Thus, the first equivalent distributed among two binding sites, V and VI, most of it as Cd_1Zn_3-αMT (Figure 6).

The second aliquot of $^{111}Cd^{2+}$ gave rise to four major peaks with chemical shifts of 651.5, 647.3, 614.7, and 613.0 ppm (Figure 5), the same set as above. The principal species was Cd_2Zn_2-αMT; minor Cd_1Zn_3-αMT (647.2 and 613.1 ppm resonances) and Cd_3Zn_1-αMT species also appeared in the spectrum at this point (peaks at 603.91, 616.09, 624.12, 639.38, 641.12, and 667.78 ppm).

The third aliquot generated a spectrum with 12 major peaks with chemical shifts of 671.5, 667.8, 651.4, 641.1, 639.4, 631.0, 626.4, 624.1, 616.1, 614.7, 611.0, and 603.9 ppm (Figure 5). These peaks were identified as 1, 3, 4, and 7−15, respectively. Peaks 4 and 13 were present in the second spectrum, representing residual Cd_2Zn_2-αMT. Peaks 7, 12, and 15 refer to a configuration with $^{111}Cd^{2+}$ bound in sites V, VI, and VII as Cd_3Zn-αMT.[11] $^{111}Cd^{2+}$ that produced peaks 3, 8, and 11 was linked to a $^{111}Cd^{2+}$ configuration involving I, V, and VI as Cd_3Zn-αMT. The remaining peaks 1, 9, 10, and 14 were associated respectively with sites I, V, VI, and VII in the final $^{111}Cd_4$-αMT configuration (Figure 6). The two peaks at 659.5 and 661.2 ppm were not identified as known metal clusters. Thus, after the third addition of $^{111}Cd^{2+}$, sites V and VI were filled and some Cd^{2+} had distributed into the other two sites, I or VII, forming Cd_3Zn_1-αMT (Figure 6).

The final equivalent of $^{111}Cd^{2+}$ resulted in four major peaks with chemical shifts of 671.5, 631.0, 626.2, and 611.0 ppm (Figure 5). As above, these four peaks were 1, 9, 10, and 14, respectively, and represented the spectrum of $^{111}Cd_4$-αMT (Figure 6). Accordingly, sites V and VI were the first to exchange with Cd^{2+}. Then, binding sites I and VII underwent substitution.

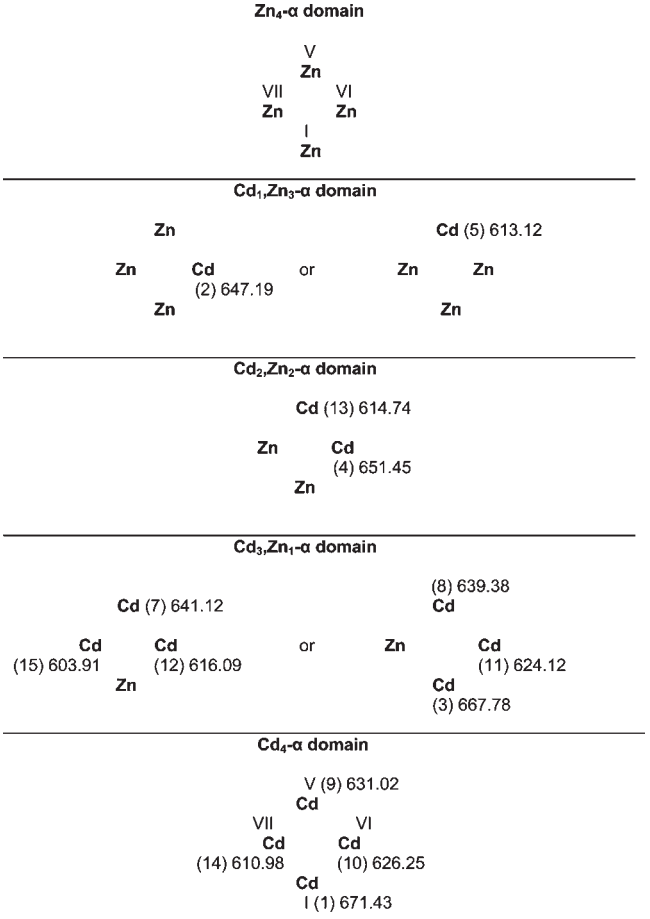

Figure 6. Schematic of the major titration pathway of the reaction of Cd^{2+} with Zn_4-αMT-2 monitored by 1-D $^{111}Cd^{2+}$ NMR. The numbered sites are the resonances labeled in Figure 5, and the Roman numerals define the connectivities of each Cd^{2+} with domain sulfhydryl groups.

Properties of Reaction of Zn_4-αMT, Zn_3Cd_1-αMT, ..., Zn_1Cd_3-αMT with Cd^{2+}. The kinetics of metal ion exchange between Zn_4-αMT, Zn_3Cd_1-αMT, ..., Zn_1Cd_3-αMT and Cd^{2+} were studied under pseudo first-order conditions to test our hypothesis that the Zn,Cd-cluster distributions approximately mirrored species formed in the different kinetic concurrent phases of the reaction of Zn_4-αMT with Cd^{2+}. The NMR titration results described above showed that there is a principal structural pathway for the $Cd^{2+}-Zn^{2+}$ exchange reaction, such that each Cd^{2+} addition yields products based on the observed rates of the concurrent phases. The faster kinetic phase results in the major metal clusters early in the titration, and other minor species along the same pathway that accumulate later in the titration are associated with the slow kinetic phase. Recognizing this complexity, we aggregated the slower steps in the analysis of the reaction kinetics of the titrated Cd_n,Zn_{4-n}-α domain species. Thus, the UV kinetic data were analyzed on the basis of a model of double concurrent pseudo first-order reactions leading to the same product, in which the slower steps were aggregated for analysis.

The percent changes in absorbance for the faster and slower phases were measured throughout a series of reactions of Zn_nCd_{4-n}-αMT with Cd^{2+} (Table 5). In the reaction of Cd^{2+} with Zn_4-αMT, two Cd^{2+} ions exchange in the fast phase (50% total absorbance change) and two

Table 5. Percent Absorbance Change Occurring in the Fast and Aggregated Two Slower Phases of Zn_m,Cd_n-αMT's Reactions with 600 μM Cd^{2+}

	percent absorbance change in exchange reaction		percent of kinetic phase filled with cadmium	
	% k_{fast}	% k_{slow}	k_{fast}	k_{slow}
Zn_4-αMT	50	50	0	0
Zn_3Cd_1-αMT	24	46	52%	8%
Zn_2Cd_2-αMT	10	35	80%	30%
Zn_1Cd_3-αMT	3	11	94%	78%
Cd_4-αMT	0	0	100%	100%

Cd^{2+} ions exchange in the aggregated slower phases (50% total change in absorbance). In comparison, the absorbance change of the fast phase of the reaction of Zn_3Cd_1-αMT with Cd^{2+} was reduced from 50% to 24% of the total change in absorbance for the reaction of Zn_4-αMT with Cd^{2+}, equivalent to binding one Cd^{2+} in the fast step. The extent of reaction in the combined slower phases was only marginally reduced from 50% to 46%. These results are consistent with the first added Cd^{2+} equivalent filling 52% of the two binding sites associated with the fast phase and 8% of the two binding sites associated with the slow phase. Therefore, it is hypothesized that the single Cd^{2+} equivalent in Zn_3Cd_1-αMT was located in a site(s) identified mostly with the fast phase of the reaction of Zn_4-αMT with Cd^{2+}.

In the reaction of Zn_2Cd_2-αMT with Cd^{2+}, the 2 Cd^{2+} equivalents in the starting structure filled 80% of the two binding sites associated with the fast phase and 30% of the two binding sites associated with the slower phases. This result supports the two phases of reaction occuring concurrently and the titrated, mixed metal species forming concurrently rather than in sequential order. Continuing this trend, the 3 Cd^{2+} equivalents in Zn_1Cd_3-αMT filled 94% of the two binding sites associated with the fast phase and 78% of the two binding sites associated with the slow phases. Thus, in this species, the two binding sites involved in the faster phase were almost filled, as was more than one equivalent of the binding sites involved in the slower phase. The cumulative kinetic behavior of these mixed metal species in the metal exchange reactions mimics the entire reaction of Zn_4-α-MT-2 with Cd^{2+}. As such, there is strong support for identifying the experimental pathway of Cd^{2+} binding into MT's metal binding sites observed in the NMR titration experiment with the hypothetical pathway of the overall reaction.

Discussion

Metal ion exchange reactions are at the core of the understanding of the role of MT in the detoxification of heavy metals. Thus, when Cd^{2+} enters the cell, it binds to any metal unsaturated MT that may be present and displaces Zn^{2+} from extant Zn-MT. In addition, it stimulates the induction of MT mRNA.[20,21] Thereafter, in one study involving the injection of rodents with a large concentration of Cd^{2+}, Cd-MT was the first detected MT species.[12] Later, mixed metal Cd,Zn-MT was observed as the final steady state product. The in vivo mixed metal species has been shown to form through a remarkable interprotein metal ion exchange between Zn_7-MT and Cd_7-MT as in reaction 2 that results in the preferential location of Cd^{2+} in the α domain and Zn^{2+} in the β domain.[11] The mechanism of this reaction has not been elucidated, although it is assumed that a bimolecular step involving the reaction of thiolates of one metal cluster with metal ions of the other mediates the exchange.[22]

A previous study of the exchange reaction between Zn_7-MT and Cd^{2+} defined the order and location of exchange among the seven Zn^{2+} binding sites.[11] Interestingly, according to Cd-NMR spectroscopy, the intermediate $Cd_nZn_{(7-n)}$-MT species are not identical to the stoichiometrically equivalent, mixed metal species formed in the interprotein exchange reaction. Indeed, when the former are heated to 50° and then cooled to room temperature, their one-dimensional Cd-NMR spectra convert to those of the corresponding mixtures derived from MT protein−protein metal ion exchange.[12] Apparently, the intermediate titration products in the reaction of Cd^{2+} with Zn_7-MT contain kinetically not thermodynamically stable metal ion distributions.

We undertook a comprehensive investigation of the kinetics of reaction of Zn_7-MT with Cd^{2+} in order to understand in mechanistic detail how this initial cellular reaction occurs. Detailed stopped-flow kinetic experiments revealed that the β and α domains display substantially different rates of reaction. Under pseudo first-order conditions for Cd^{2+}, the Zn_3S_9 cluster reacts more rapidly with Cd^{2+} than any of the Zn^{2+} sites in the α domain cluster and forms the homologous Cd_3S_9 cluster in a single kinetic step characterized by a second order rate constant of 7.5×10^4 M^{-1} s^{-1} at 25 °C (Table 2). For the reaction to be first order in Cd^{2+} and cluster as shown in Table 3 and for this reaction to follow the same kinetics when the rates of Cd−sulfhydryl bond formation (254 nm absorbance) and Zn^{2+} displacement (Zn-zincon formation) are observed suggests that the overall reaction

$$Zn_3S_9 + 3Cd^{2+} \rightleftharpoons Cd_3S_9 + 3Zn^{2+} \quad (11)$$

is rate limited by the exchange of the first Cd^{2+} and Zn^{2+}

$$Zn_3S_9 + Cd^{2+} \rightleftharpoons Cd,Zn_2S_9 + Zn^{2+} \quad (12)$$

The question arises why the reactions of Cd^{2+} with Cd,Zn_2,S_9 or Cd_2,Zn,S_9 should be non-rate-limiting. One hypothesis is that the rapid rate of intersite metal ion exchange in the β domain cluster distributes the bound Cd^{2+} among all of the sites so that Cd^{2+} can enter the cluster by the same route in each reaction. However, the $Cd^{2+}-Cd^{2+}$ intersite exchange rate constants at 35 °C range from 0.2 to 2.7 s^{-1}, far smaller than the pseudo first-order rate constants for the three phases of the metal exchange reaction (17−180 s^{-1}).[22] More likely, the β domain metal ion rates are so fast that differential rate behavior cannot be observed.

The observed reaction of Cd^{2+} with Zn_4S_{11} in the α domain is considerably more complex, perhaps because the β domain reaction rates are so fast that differential rate behavior cannot be observed. The overall process is comprised of three sequential or concurrent steps, each displaying saturation behavior consistent with reversible binding of

(20) Durnam, D. M.; Palmiter, R. D. *J. Biol. Chem.* **1981**, *256*, 5712–5716.
(21) Glanville, N.; Durnam, D. M.; Palmiter, R. D. *Nature* **1981**, *292*, 267–269.
(22) Otvos, J. D.; Liu, X.; Li, H.; Shen, G.; Basti, M. *Metallothionein III: Biological Roles and Medical Implications*; Suzuki, K. T.; Imura, N.; Kimura, M.; Birkhäuser Verlag: Basel, Switzerland, 1993; pp 57−74.

Cd^{2+} to the protein followed by intramolecular $Cd^{2+}-Zn^{2+}$ exchange as in reaction 14.

$$Zn_4\text{-}\alpha + Cd^{2+} \rightleftharpoons Cd\cdot Zn_4\text{-}\alpha \quad (13)$$

$$Cd\cdot Zn_4\text{-}\alpha \rightleftharpoons Cd, Zn_3\text{-}\alpha + Zn^{2+} \quad (14)$$

It is hypothesized that the slow intersite metal ion exchange rate within the α domain results in each site retaining individual kinetic properties (Tables 1 and 2).[22] According to this mechanism and the interpretation made in relation to reactions 5−7, observation of the formation of the product species (254 nm absorbance) and Zn^{2+} availability to react with zincon should and do yield the same rate of reaction. The small K_d values for reaction 13, ranging from 2 to 9 mM at 25°, are consistent with weak adduct formation between cluster thiolate groups and Cd^{2+}. The formation of Cd^{2+} adducts with Cd_n,Zn_{4-n}-MT as intermediates along the metal ion exchange pathway is also supported by a recent study in which NMR experiments supported the formation of a Cd_5-αMT species that might be construed as $Cd\cdot Cd_4$-αMT species.[23]

In light of the results with the α domain, we propose that the reaction of Cd^{2+} with the β domain occurs by the same mechanism. The lack of any indication of binding in the Cd^{2+} dependence of the reaction would be consistent with K_d values greater than 10 mM for the β domain reaction such that eq 7 reduces to

$$k_{obs} = k[Cd^{2+}]/K_d \quad (15)$$

under the conditions of the reactions.

Experiments compared the reaction of Cd^{2+} with the Zn_4-α domain to that of Cd^{2+} with Cd species (Cd_1,Zn_3-αMT, Cd_2Zn_2-αMT, and Cd_3Zn_1-αMT) generated in the titration of Zn_4-αMT with Cd^{2+} that are hypothetical intermediates in the reaction of the Zn_4-α domain with Cd^{2+}. Supporting the use of structural results determined at millimolar protein concentrations with kinetic studies done at micromolar concentrations was our previous structure−reactivity study comparing the structures of the isolated Cd_4-α domain with the Cd_4-α domain in Cd_7-MT.[19] They differ in conformation, with the isolated domain displaying larger thiolate solvent accessibility than the holoprotein that exists as a dimer at millimolar concentrations. The dimer, forming along the $\alpha-\beta$ interface, only exists with the holoprotein. In turn, the holoprotein but not the isolated domain reacts differently with EDTA in the two concentrations regimes. By inference, the structures of the Zn,Cd-domain species should be representative of the structures present in the kinetic studies.

The kinetic results with the mixed metal species were consistent with Cd^{2+} undergoing a set of three independent reactions with the α domain cluster to form Cd_4-αMT, which displayed the same qualitative kinetic behavior as the individual steps of the reaction of Zn_4-αMT. $^{111}Cd^{2+}$ NMR spectroscopy of the prepared intermediate species was consistent with results of a previous study and demonstrated that the fast kinetic phase binding Cd^{2+} primarily entered cluster sites V and VI to form Cd_2Zn_2-αMT. The slower kinetic phases largely populated sites I and VII to yield Cd_4-αMT. Therefore, the combination of kinetic and structural experiments were consistent with the identification of the fastest kinetic step with the exchange of Cd^{2+} with Zn^{2+} in sites V and VI and the two slower steps with the population of sites I and VII with Cd^{2+} (Figure 6). Accordingly, the kinetics can be characterized as a set of concurrent reactions of Cd^{2+} with different metal ion binding sites in the cluster.

Table 6. Cd + α Domain Cysteinyl Sulfhydryl Solvent Accessibility

Cd site	cysteinyl sulfur ligands[a]	sulfur atom accessible surface (Å^2)[b]
Cd_I	**50**, *57*, *59*, **60**[c]	18
Cd_V	*33*, ***34***, **44**, *48*	17
Cd_{VI}	***37***, *41*, **44**, **60**	12
Cd_{VII}	***34***, *36*, ***37***, 50	12

[a] Reference 5. [b] Reference 19. [c] Bold, bridging ligands; italics, surface accessible sulfurs.

The Cd^{2+}-domain adduct formation reactions that initiate each kinetic step (reactions 5 and 13) are envisioned to involve the interactions of the metal ion with thiolate groups that are also ligated to Zn^{2+} within the $Cd_n,Zn_{4-n}S_{11}$ cluster. Cysteine sulfhydryl groups that might participate in these reactions would be those that are solvent accessible and provide access to the cluster. An examination of the NMR structure of Cd_4-αMT-2 revealed that most of the thiolate ligands display some solvent accessibility (Table 6).[19] The domain crevice contains four accessible sulfurs, one from site I (C57, 6 Å^2 surface accessible area, terminal sulfhydryl group) and two from sites VI (C37, 6 Å^2, bridging; C41, 6 Å^2, terminal) and VII (C36, 3 Å^2, terminal; C37). Another region of the surface contains cysteines 34 (3.5 Å^2, bridging) and 48 (9 Å^2, terminal) associated with metal ion VI. Several individual sulfur atoms from cysteines 33 (site V, 3.5 Å^2, terminal), 41 (VI), and 59 (I, 9.5 Å^2, terminal) are also exposed to the solvent.

This information suggests the following pathway of reaction (Figure 7). Cd^{2+} readily reacts with the dithiol sites, C37−C41 (site VI) or C34−C48 (V), to form intermediate Cd^{2+}-cluster adducts that in either case involve a bridging and a terminal thiolate sulfur. Which of these pairs of sulfhydryl groups favors the entrance and distribution of both Cd^{2+} ions into sites V and VI has not been ascertained. Perhaps, both are utilized and cannot be kinetically distinguished. Subsequently, sites VII and I are accessed through sulfurs from residues C36 and C37 and C57 or C59, respectively.

The activation parameters for the subsequent exchange steps (Table 4) considered in conjunction with Figure 7 suggest some additional features of the pathway. Considering the sequential replacement of Zn^{2+} by Cd^{2+} and the substantially greater stability of Cd−S bonding than its Zn−S counterpart, it is plausible that the trend of increasing $\Delta H^{\ddagger}$ represents the progressively greater difficulty in breaking Zn−sulfhydryl bonds as the intermediate adduct species, $Cd\cdot(Cd_n,Zn_{4-n}\text{-}\alpha)$, undergoes reaction. The trend might also reflect the fact that both sites I and VII contain CXCC amino acid/ligand sequences, which may comprise particularly powerful arrays of chelating sulfhydryl groups. In particular, site I is the only metal binding site in which four consecutive thiolates in the sequence bind to the same metal ion and might be identified with k_3.[23]

(23) Rigby Duncan, K. E.; Kirby, C. W.; Stillman, M. J. *FEBS J.* **2008**, *275*, 2227−2239.
(24) Muñoz, A.; Laib, F.; Petering, D. H.; Shaw, C. F., 3rd *J. Biol. Inorg. Chem.* **1999**, *4*, 495–507.

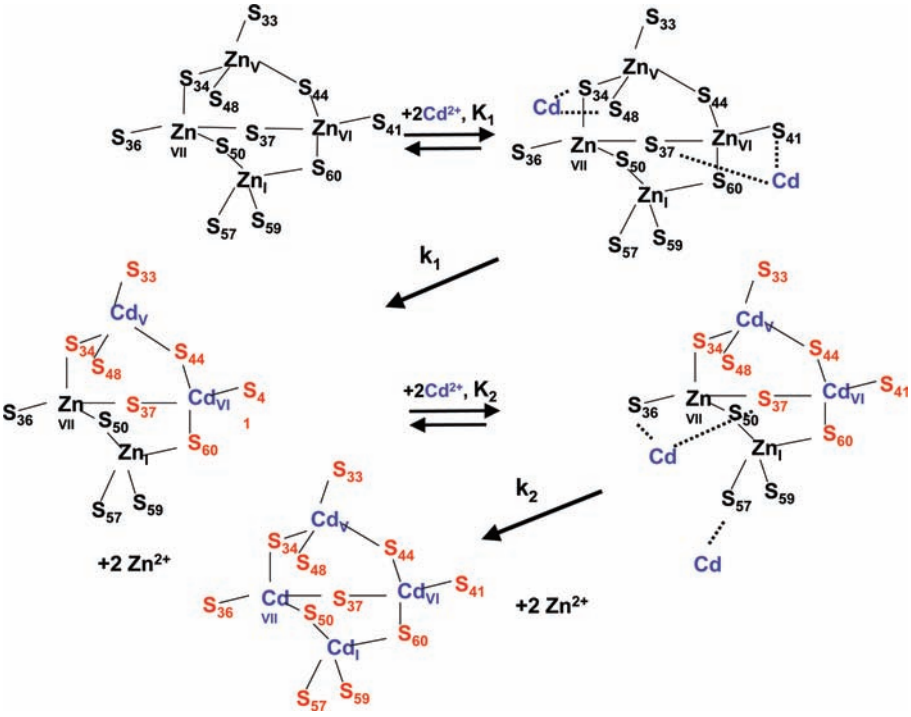

Figure 7. Hypothetical mechanistic pathway of the reaction of Cd^{2+} with Zn_4-αMT-2.

The increasing trend in $\Delta S^{\ddagger}$ may also reflect the same differential structural characteristic of the sites. Thus, the CXCC features would allow relatively little peptide flexibility during the exchange process when metal−thiolate bonds are broken and remade. In contrast, during the reactions of sites V and VI, the X_n sequences of amino acids between cysteinyl residues may introduce a greater opportunity for flexibility during rate limiting bond making and breaking, requiring less structural reorganization.

The model of the reaction of Cd^{2+} with the Zn_4-α domain may now be considered in light of the titration of Zn_7-MT with Cd^{2+} studied previously by $^{111}Cd^{2+}$ NMR spectroscopy.[11] As described above, in the kinetic experiments conducted at micromolar concentrations, Cd^{2+} reacts fastest with Zn_3-β and, accordingly, populates the β domain faster than the α domain. However, in the full NMR titration experiment done with millimolar concentrations of reactants, the observed distribution of $^{111}Cd^{2+}$ follows the sequence Cd_1(site III-β), Cd_{2-5}(sites I, V, VI, VII-α), and $Cd_{6,7}$(sites II, IV-β).[11] The fact that the α domain fills with Cd^{2+} before two of the three β domain binding sites suggests that interprotein $Cd^{2+}-Zn^{2+}$ exchange takes place to move Cd^{2+} initially bound in the β domain into the α domain. Under the conditions of the NMR experiment (mM MT concentration), much of the protein exists as a dimer, based on its K_d of 400:M.[19,22] Dimerization is also thought to be a key step in the interprotein metal ion exchange reaction between Cd_7-MT and Zn_7-MT.[22]

The sequence of Cd^{2+} replacement listed above implicates β domain sites II and IV as the Cd^{2+} donor sites. Presumably, α domain sites V and VI are the initial acceptor sites. This locus of metal ion exchange could invoke the hypothetical interface of the metallothionein dimer as revealed in the crystal structure and supported in a recent NMR comparison of the holoprotein and α domain structures.[6,19] According to those studies, α and β domains and surface accessible thiols 41 (site VI, α) and 44 (V, VI,α) and 19 (II, β) and 21 (IV,β) lie in proximity at the α−β interface. It is envisioned that metal−thiolate sites in each domain exchange sulfhydryl ligands as the starting point for metal ion exchange.

$$(Cd_3S_9) + (Zn_4S_{11}) \rightleftharpoons (Cd_3S_9)\cdot(Zn_4S_{11}) \qquad (16)$$

$$(Cd_3S_9)\cdot(Zn_4S_{11}) \rightleftharpoons (Zn_m, Cd_{3-m}S_9)\cdot(Cd_n, Zn_{4-n}S_{11}) \qquad (17)$$

$$(Zn_m, Cd_{3-m}S_9)\cdot(Cd_n, Zn_{4-n}S_{11}) \rightleftharpoons (Zn_m, Cd_{3-m}S_9) + (Cd_n, Zn_{4-n}S_{11}) \qquad (18)$$

Conceptually, this process closely resembles the metal ion exchange mechanism proposed for the reaction of Cd^{2+} with Zn_7-MT.

Acknowledgment. The authors acknowledge the support of NIH grants ES-04026 and ES-04184.

Supporting Information Available: Five additional figures showing metal exchange reactions and plots of k_{obs} versus ion concentrations. This material is available free of charge via the Internet at http://pubs.acs.org.